

## Light Scattering near the Localization Transition in Macroporous GaP Networks

Frank J. P. Schuurmans,<sup>1</sup> Mischa Megens,<sup>1</sup> Daniël Vanmaekelbergh,<sup>2</sup> and Ad Lagendijk<sup>1</sup>

<sup>1</sup>*Van der Waals-Zeeman Instituut, Universiteit van Amsterdam, Valckenierstraat 65, 1018 XE Amsterdam, The Netherlands*

<sup>2</sup>*Debye Instituut, Universiteit Utrecht, P.O. Box 80000, 3508 TA Utrecht, The Netherlands*

(Received 12 March 1999)

We studied enhanced backscattering of light from anodically and photoanodically etched, macroporous GaP networks. The most strongly scattering material for visible light reported to date, photoanodically etched GaP, features anomalous rounding of the top of the backscatter cone. The phenomenon cannot be attributed to finite sample size or absorption and is most likely the onset of Anderson localization.

PACS numbers: 42.25.Dd, 42.25.Hz, 42.70.Qs, 78.55.Mb

It is well established that the properties of light in multiply scattering media are affected by interference. Important examples are enhanced backscattering [1], short and long-range correlations in the intensity fluctuations [2], universal conductance fluctuations [3], and Anderson localization [4–6]. To observe these phenomena in full glory, light should be elastically scattered, meaning that light absorption must be negligible. For Anderson localization, i.e., inhibition of light propagation due to interference, the material should also be extremely strongly scattering. That is, the transport mean free path, the average distance light propagates before its direction is randomized, should be of the order of the wavelength of light. Such strong scattering can be attained only for large relative variations in refractive index on the length scale of the wavelength. For years, these requirements could not be met for visible light. Only for microwave radiation localization effects were observed [7].

Quite recently a new route towards Anderson localization was worked out, using high refractive index semiconductors in the nonabsorbing, subband gap region. For finely grained GaAs powders, the first observation of strong localization of near infrared light has been reported [6].

Exploiting photo-assisted electrochemical etching techniques, we have made a new type of strongly scattering material: macroporous GaP networks [8]. GaP has a large refractive index of  $\sim 3.3$  and an indirect band gap of 2.24 eV (550 nm) [9], making it a good candidate for preparing a material which features Anderson localization in the red part of the visible spectrum. Macroporous GaP is the most strongly scattering medium for visible light reported to date, and localization effects are anticipated.

In this Letter, we present measurements of enhanced backscattering of these strongly scattering materials, as enhanced backscattering is expected to be very sensitive to Anderson localization [10]. We used two types of macroporous GaP: anodically (A-GaP) and photoanodically (PA-GaP) etched GaP [8]. For the stronger scattering material, PA-GaP, we observe an anomalous rounding of the en-

hanced backscatter cone. The effect of finite sample sizes is investigated. The contribution of absorption is studied by filling the pores with dielectric material. Both finite sample size and absorption are eliminated as possible sources for the observed extra cone rounding. The phenomenon cannot be described by classical light diffusion and is most likely the onset of Anderson localization.

The materials are random networks of single crystalline GaP with pore sizes of  $\sim 150$  nm and porosities of 35 and 50% for A-GaP and PA-GaP, respectively [8]. Accordingly, the effective refractive indices  $n_e$  [11,12] are  $2.0 \pm 0.1$  (A-GaP) and  $1.7 \pm 0.1$  (PA-GaP). The porous slab thicknesses range from 5 to 120  $\mu\text{m}$  for A-GaP and from 5 to 60  $\mu\text{m}$  for PA-GaP [13]. From total transmission measurements at a wavelength  $\lambda$  of 685 nm [8],  $k_e\ell$ -values were inferred using classical diffusion theory [14,15] taking into account internal reflection corrections [11,12,16]. Here  $k_e = \frac{2\pi}{\lambda}n_e$  is the wave vector in the medium and  $\ell$  the transport mean free path. For A-GaP we found  $k_e\ell = 8.6 \pm 0.5$  and for PA-GaP  $k_e\ell = 2.6 \pm 0.2$ , making the latter the most strongly scattering material for visible light. The transmission measurements show no signs of absorption for both types of material, leading to the conclusion that the (diffuse) absorption length  $L_a$  is considerably larger than the thickest samples, that is  $L_a \geq 150 \mu\text{m}$  for A-GaP and  $L_a \geq 80 \mu\text{m}$  for PA-GaP.

The enhanced backscatter cones are recorded using the off-centered rotation technique [17]. The accessible angular range is large, 0.9 rad, which is necessary to accurately measure the broad wings of backscatter cones of very strongly scattering samples. The large illumination area of 4 mm in diameter results in a resolution better than 0.4 mrad, enabling precise investigation of the top of the cone. The measurements are performed at  $\lambda = 685$  nm allowing direct comparison with transmission data [8]. Ensemble averaging is performed by spinning the sample [17]. Linearly polarized light was used to illuminate the samples and the detection was in the polarization-conserving channel [18]. For these polarization channels also single scattered light is detected, effectively raising the diffuse background [19]. As a result the enhancement

factors of the backscatter cones are not equal to 2. This does not affect our further results.

Figure 1 shows the backscattered intensity of our two materials, A-GaP and PA-GaP. The backscattered intensity exhibits a pronounced peak, which arises from constructive interference of time-reversed light scattering paths in the backscattering direction. Short light paths interfere over a considerable range of angles, whereas very long light paths interfere only in exact backscattering. The result is a triangular peak superimposed on the diffuse backscattered intensity [20,21], known as the enhanced backscatter cone. The width of the cone is determined by the length of the light paths, i.e., by the transport mean free path. The much broader cone of PA-GaP immediately reflects the stronger scattering of this material. In order to quantitatively determine  $k_e \ell$  from these measurements, internal reflection must be taken into account. The diffuse reflection coefficient  $R$  of the sample-air interface depends on the effective refractive index of the scattering material  $n_e$  [12], giving  $R = 0.78 \pm 0.05$  for A-GaP and  $R = 0.67 \pm 0.06$  for PA-GaP. From the full width at half maximum  $W$  of the cone and using  $k_e \ell \approx 0.7n_e W^{-1}(1 - R)$  [12,21], we find that for A-GaP  $k_e \ell = 10.6 \pm 0.9$  and for PA-GaP  $k_e \ell = 3.2 \pm 0.4$ . These values are in good agreement with the transmission results, establishing PA-GaP as the most strongly scattering material for visible light reported to date.

Filling the pores of PA-GaP with 1-dodecanol, which is nonabsorbing and has a refractive index of  $\sim 1.44$ , lowers the refractive index contrast, resulting in less strong scattering; see Fig. 2. This is the first measurement of enhanced backscattering where the effect of refractive index contrast has been investigated for one microscopic

scattering realization of the disorder. The alcohol has a convenient melting point of  $\sim 26^\circ\text{C}$  just above room temperature, allowing to fill the samples with liquid and perform the backscatter cone measurements in the solid phase. During the filling procedure the light transmission intensity [8] is monitored in order to ensure complete filling. As a result of this filling, the full width at half maximum of the cone narrows by a factor  $2.1 \pm 0.1$ , corresponding to an increase in  $k_e \ell$  [22]. The observed increase in  $k_e \ell$  with a factor of  $2.1 \pm 0.1$  is in excellent agreement with the increase of transmission upon filling, which is  $2.20 \pm 0.05$  [8].

Normally the top of the enhanced backscatter cone is cusped, resulting from interference of infinitely long light paths. However, close to and in the Anderson localization regime the top of the backscatter cone is expected to be rounded [10], as especially the long light paths are affected by localization [4,5]. Inspection of the observed top reveals a clear rounding; see Fig. 3. It should be noted that the enhanced backscatter cone can also have a rounded top in the classical regime: absorption [15,21,23,24] and finite sample size [15,21,24,25] present a cutoff on long light paths, which therefore cannot contribute to enhanced backscattering. It is thus essential to study the influence of absorption and finite sample thickness, in order to clearly reveal Anderson localization.

To investigate this rounding quantitatively, we introduce a convenient measure of cone rounding that is easily extracted from the data. We define the rounding  $\Delta\Theta_R$  as follows: First the wings of the measured enhanced backscatter cone are extrapolated into a triangular cone, representing the cone with no cutoff on long light paths.

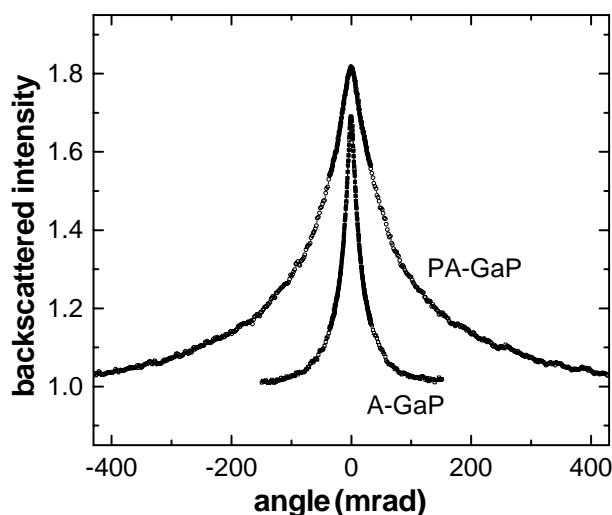


FIG. 1. The backscattered intensity normalized to the diffuse background as a function of angle for anodically (A-GaP) and photoanodically (PA-GaP) etched GaP. From the width of the cone, incorporating internal reflection corrections, the  $k_e \ell$  values are inferred. The narrow cone: A-GaP,  $k_e \ell = 10.6 \pm 0.9$ . The broad cone: PA-GaP,  $k_e \ell = 3.2 \pm 0.4$ .

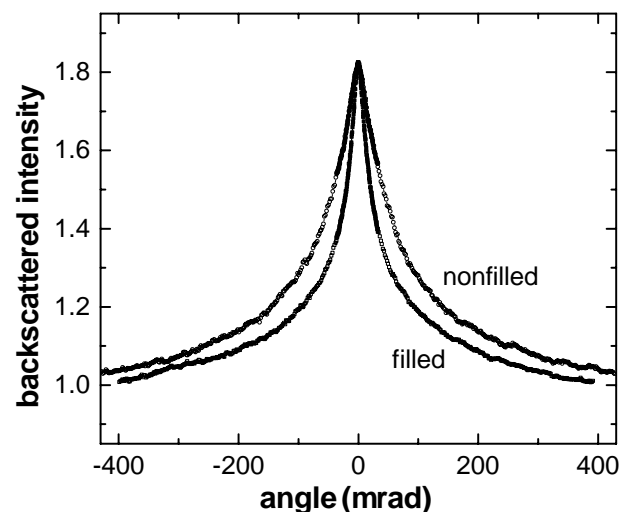


FIG. 2. The backscattered intensity normalized to the diffuse background as a function of angle for photoanodically etched GaP (PA-GaP) and exactly the same sample filled with 1-dodecanol. Because of the decrease in refractive index contrast, the scattering efficiency of filled PA-GaP is lower, reflected by the narrower cone. The cone of nonfilled PA-GaP is a factor of  $2.1 \pm 0.1$  broader than the filled one.

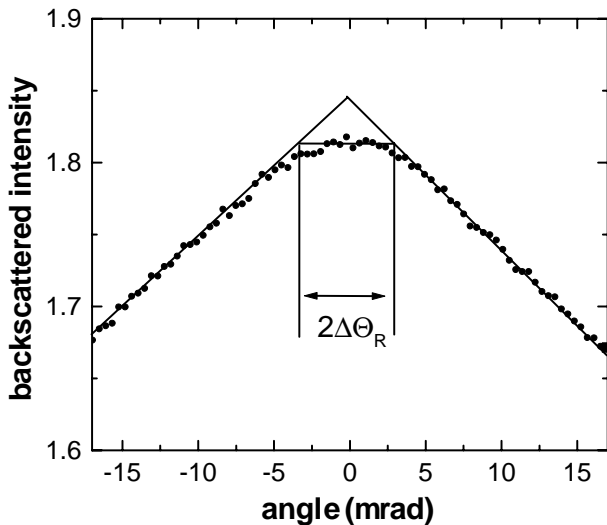


FIG. 3. The top of the enhanced backscatter cone of  $60 \mu\text{m}$  thick photoanodically etched GaP showing a clear rounding.  $\Delta\Theta_R$  is the measure of cone rounding as defined in the text. Here  $\Delta\Theta_R$  is  $3.4 \pm 0.2$  mrad.

Then,  $2\Delta\Theta_R$  is taken to be the width of the cusped cone at the height of the rounded cone; see Fig. 3. This definition is independent of the enhancement factor. In the classical diffusion regime with absorption length  $L_a$  and sample thickness  $L$ , small cone roundings ( $\Delta\Theta_R \ll W$ ) can be derived from an explicit formula for the line shape of enhanced backscattering [21]

$$\Delta\Theta_R = \frac{1}{kL_a} \coth\left(\frac{L_e}{L_a}\right). \quad (1)$$

Here  $L_e = L + 2z_e$  is the effective sample thickness and  $z_e$  the extrapolation length that depends on the internal reflection coefficient  $R$  and is of the order of  $\ell$  [12]. If  $L_e \gg L_a$ , the rounding is solely determined by absorption:  $\Delta\Theta_R = 1/(kL_a)$ . On the contrary, for  $L_e \ll L_a$  the rounding is due to the finite sample size:  $\Delta\Theta_R = 1/(kL_e)$ . These findings agree with previous derivations [15,23–25]. The fact that Eq. (1) is not symmetric in  $L_e$  and  $L_a$  reflects the physical difference between path length cutoff due to finite sample size and due to absorption, which are deterministic and probabilistic, respectively [15].

To distinguish the possible mechanisms for cone rounding, we have measured enhanced backscatter cones for various sample thicknesses  $L$ . The cone roundings  $\Delta\Theta_R$  of A-GaP, PA-GaP, and PA-GaP filled with 1-dodecanol are given in Fig. 4. Clearly, the cone roundings of A-GaP and filled PA-GaP follow  $\Delta\Theta_R = 1/kL_e$ , and hence can be fully explained by the finite sample thickness. Absorption plays no role for these two types of samples:  $L_a \gg L_e$ , in agreement with transmission measurements. In contrast, the cone roundings of nonfilled PA-GaP do not tend to zero for thick samples,  $1/kL_e \downarrow 0$ . Attempting to interpret this extra cone rounding of PA-GaP as the contribution of absorption, we use Eq. (1) to describe the measurements, resulting in a tentative absorption length  $L'_a$

of  $33 \pm 2 \mu\text{m}$ . This contradicts the transmission measurements from which we concluded that  $L_a \geq 80 \mu\text{m}$ . Moreover, it is also at variance with the observed cone roundings of filled PA-GaP: If the extra cone rounding of nonfilled PA-GaP originates from absorption, then filled PA-GaP also absorbs light and hence would likewise show extra cone rounding, which is evidently not the case as the cone roundings of filled PA-GaP follow the straight line in Fig. 4. This discrepancy can be made more quantitative using  $L_a = \sqrt{\ell_a \ell}/3$  known from diffusion theory [14], where  $\ell_a$  is the material absorption length and  $\ell$  the transport mean free path. Filling increases  $\ell$  (see Fig. 2), but leaves  $\ell_a$  unaffected. Consequently, from the tentative absorption length of  $33 \mu\text{m}$  for nonfilled PA-GaP, we find that  $L_a$  for filled PA-GaP should be  $\sqrt{2.1} \times 33 \mu\text{m} \approx 48 \mu\text{m}$ . Comparison of the theoretical curve for this absorption length [Eq. (1)] with the data for filled PA-GaP shows that an interpretation in terms of absorption fails; see Fig. 4. Therefore, we have shown independently that the extra cone rounding for PA-GaP cannot be explained by either absorption or finite sample size.

The effect of extra cone rounding of PA-GaP can be switched off by filling the sample with 1-dodecanol, decreasing the scattering efficiency. Apparently, the extra cone rounding is only observed for the strongest scattering material, closest to the localization transition: the phenomenon is most likely an effect of Anderson localization. Pioneering theoretical work [10] on enhanced

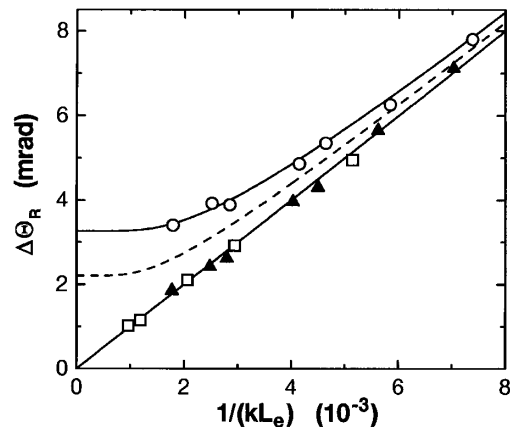


FIG. 4. The cone roundings  $\Delta\Theta_R$  of anodically etched GaP (A-GaP, open squares), photoanodically etched GaP (PA-GaP, open circles), and PA-GaP filled with 1-dodecanol (filled triangles) as a function of inverse effective sample thickness. The solid straight line is the theoretical prediction from Eq. (1) assuming that absorption is negligible ( $L_a \gg L_e$ ), using no adjustable parameters. PA-GaP shows extra rounding for thick samples and is compared to Eq. (1), where  $L'_a = 33 \pm 2 \mu\text{m}$  (solid curved line). The dashed curve comes from Eq. (1) with  $L'_a = 48 \mu\text{m}$ , the absorption length predicted for filled PA-GaP using diffusion theory and the data for nonfilled PA-GaP. Clearly, the dashed curve does not describe the measured cone roundings for PA-GaP filled with 1-dodecanol, excluding absorption as a source for the extra cone rounding of nonfilled PA-GaP. The error bars are of the order of the symbol size.

backscattering off a semi-infinite medium close to localization, with coherence length  $\xi$  [5], indeed predicts a modified top of the cone: the slope at zero angle is determined by the renormalized transport mean free path  $\ell(\ell/\xi)$ , instead of  $\ell$  [20] ( $\xi = \ell$  in the classical limit). The wings of the backscatter cone are hardly affected by localization, as the corresponding short light scattering paths are not renormalized [5]. Upon approaching localization ( $\xi$  going from  $\ell$  to  $\infty$ ), the top of the cone becomes less cusped and ultimately parabolic (rounded); a small discontinuity of the slope is experimentally difficult to observe. In our experiments, the predicted weakly cusped cone of a semi-infinite medium is not observed; the measured cones are rounded. This is probably caused by the finiteness of even our thickest samples. Although qualitatively the existing localization theories [10] describe the experiment, a quantitative comparison cannot be made. For example, diffuse internal reflection [11,12] in combination with scaling theory of localization has not yet been studied. As it is essential to consider diffuse internal reflection for a quantitative description of enhanced backscattering in the classical diffusion regime, we expect it to be equally important in the localization regime.

It is remarkable that we still observe the linear dependence of the total transmission with inverse sample thickness, a hallmark of classical diffusion [4,14], whereas in enhanced backscattering the onset of localization is presumably already detected. In this respect, it should be stressed that in enhanced backscattering the angular distribution of backscattered light for different sample thicknesses is measured, whereas in total transmission only the thickness is varied. Consequently, transmission measurements give less information on the path length distribution and hence on localization, indicating that enhanced backscattering is the more sensitive probe.

In conclusion, we have measured enhanced backscattering of A-GaP, PA-GaP, and PA-GaP filled with 1-dodecanol. From the width of backscatter cones it is inferred that  $k_e \ell = 10.6 \pm 0.9$  for A-GaP and  $k_e \ell = 3.2 \pm 0.4$  for PA-GaP, making the latter the most strongly scattering material for visible light reported to date. The rounding of the top of the cone was accurately investigated. For A-GaP and filled PA-GaP it is found that the rounding can be fully described by the finite sample size, indicating that absorption is negligible. For the most strongly scattering samples, PA-GaP, we observe an extra cone rounding, which cannot be attributed to the finite sample size or absorption and is most likely due to Anderson localization.

The authors would like to acknowledge J. Gómez Rivas, G. van Soest, P. de Vries, and D. Wiersma for valuable discussions, and Philips Research Laboratories (Eindhoven, the Netherlands) for kindly supplying the GaP crystals. This work is part of the research program of the "Stichting voor Fundamenteel Onderzoek der Materie," which is financially supported by the "Nederlandse Organisatie voor Wetenschappelijk Onderzoek."

- [1] Y. Kuga and A. Ishimaru, *J. Opt. Soc. Am. A* **8**, 831 (1984); M.P. van Albada and A. Lagendijk, *Phys. Rev. Lett.* **55**, 2692 (1985); P.E. Wolf and G. Maret, *ibid.* **55**, 2696 (1985).
- [2] I. Freund, M. Rosenbluh, and S. Feng, *Phys. Rev. Lett.* **61**, 2328 (1988); N. Garcia and A.Z. Genack, *ibid.* **63**, 1678 (1989); M.P. van Albada, J.F. de Boer, and A. Lagendijk, *ibid.* **64**, 2787 (1990).
- [3] F. Scheffold and G. Maret, *Phys. Rev. Lett.* **81**, 5800 (1998).
- [4] P.W. Anderson, *Phys. Rev.* **109**, 1492 (1958); *Philos. Mag. B* **52**, 505 (1985); S. John, *Phys. Rev. Lett.* **53**, 2169 (1984); *Phys. Today* **44**, No. 5, 32 (1991).
- [5] E. Abrahams, P.W. Anderson, D.C. Licciardello, and T.V. Ramakrishnan, *Phys. Rev. Lett.* **42**, 673 (1979).
- [6] D.S. Wiersma, P. Bartolini, A. Lagendijk, and R. Righini, *Nature (London)* **390**, 671 (1997).
- [7] N. Garcia and A.Z. Genack, *Phys. Rev. Lett.* **66**, 1850 (1991); A.Z. Genack and N. Garcia, *ibid.* **66**, 2064 (1991).
- [8] F.J.P. Schuurmans, D. Vanmaekelbergh, J. van de Lage-maat, and A. Lagendijk, *Science* **284**, 141 (1999).
- [9] D.E. Aspnes and A.A. Studna, *Phys. Rev. B* **27**, 985 (1983).
- [10] R. Berkovits and M. Kaveh, *Phys. Rev. B* **36**, 9322 (1987); I. Edrei and M.J. Stephen, *ibid.* **42**, 110 (1990).
- [11] A. Lagendijk, R. Vreeker, and P. de Vries, *Phys. Lett. A* **136**, 81 (1989).
- [12] J.X. Zhu, D.J. Pine, and D.A. Weitz, *Phys. Rev. A* **44**, 3948 (1991).
- [13] The thickness of the porous structure is proportional to the anodic charge in the etching procedure, enabling precise coulometric control of this important parameter.
- [14] A. Ishimaru, *Wave Propagation and Scattering in Random Media* (Academic, New York, 1978), Vols. I and II; A.Z. Genack, *Phys. Rev. Lett.* **58**, 2043 (1987).
- [15] P. Sheng, *Introduction to Wave Scattering, Localization, and Mesoscopic Phenomena* (Academic, San Diego, 1995).
- [16] P.M. Saulnier and G.H. Watson, *Opt. Lett.* **17**, 946 (1992).
- [17] D.S. Wiersma, M.P. van Albada, and A. Lagendijk, *Rev. Sci. Instrum.* **66**, 5473 (1995).
- [18] The circular polarization channel was not used, as for our large angular range the required quarter-wave plate causes undesired polarization mixing [17].
- [19] S. Etamad, R. Thompson, and M.J. Andrejco, *Phys. Rev. Lett.* **57**, 575 (1986).
- [20] E. Akkermans, P.E. Wolf, and R. Maynard, *Phys. Rev. Lett.* **56**, 1471 (1986).
- [21] M.B. van der Mark, M.P. van Albada, and A. Lagendijk, *Phys. Rev. B* **37**, 3575 (1988).
- [22] Although the effective refractive index  $n_e$  slightly increases upon filling, the decrease in width of the backscatter cone matches the increase in  $k_e \ell$ , as correspondingly the diffuse reflection coefficient  $R$  also increases.
- [23] P.E. Wolf, G. Maret, E. Akkermans, and R. Maynard, *J. Phys. (Paris)* **49**, 63 (1988).
- [24] S. Etamad *et al.*, *Phys. Rev. Lett.* **59**, 1420 (1987).
- [25] I. Edrei and M. Kaveh, *Phys. Rev. B* **35**, 6461 (1987).